frontiers | Frontiers in Earth Science

TYPE Original Research
PUBLISHED 25 May 2023
DOI 10.3389/feart.2023.1078703

OPEN ACCESS

EDITED BY
Maria Da Glória Garcia,
University of São Paulo, Brazil

REVIEWED BY
Luis Gago-Duport,
University of Vigo, Spain
Bo Wang,
Chinese Academy of Sciences (CAS), China

*CORRESPONDENCE
Li Lo,
lilo115@ntu.edu.tw

RECEIVED 24 October 2022
ACCEPTED 10 May 2023
PUBLISHED 25 May 2023

CITATION
Pang C-H, Yang T-R, Chang Y-J, Lin S-H, Shiau L-J, Chen C-T, Chang C-P and Lo L (2023), The first discovery of amber resin in Lichi Mélange, Eastern Taiwan. *Front. Earth Sci.* 11:1078703. doi: 10.3389/feart.2023.1078703

The first discovery of amber resin in Lichi Mélange, Eastern Taiwan

Chi-Hsiu Pang[1,2], Tzu-Ruei Yang[3,4], Ying-Ju Chang[5], Shu-Hong Lin[6,7], Liang-Jian Shiau[8], Chih-Tung Chen[9], Chung-Pai Chang[9,10] and Li Lo[1,10]*

[1]Department of Geosciences, National Taiwan University, Taipei, Taiwan, [2]Institute of Earth Sciences, Academia Sinica, Taipei, Taiwan, [3]Department of Geology, National Museum of Natural Science, Taichung, Taiwan, [4]Department of Life Sciences, National Chung Hsing University, Taichung, Taiwan, [5]Institute of Earth Sciences, National Ocean University, Keelung, Taiwan, [6]Taiwan Union Lab of Gem Research (TULAB), Taipei, Taiwan, [7]Exploration and Development Research Institute, CPC Corporation, Miaoli, Taiwan, [8]Department of Earth Sciences, National Central University, Taoyuan, Taiwan, [9]Center for Space and Remote Sensing Research, National Central University, Taoyuan, Taiwan, [10]Research Center for Future Earth, National Taiwan University, Taipei, Taiwan

Amber is fossilized tree resin produced by the metabolism of vascular plants that has experienced various geological processes, including burial, compression, and heating. Therefore, most of the previously reported amber pieces were unearthed from sedimentary rocks. The record of amber in tectonic active regions, e.g., Taiwan, is extremely poor and has not been scientifically certified, leading to a poor understanding of the history of prehistoric flora in this region. This study reports a 1-cm yellow-brown amorphous resin interspersed in sandstone blocks in the Lichi Mélange at the southernmost tip of the Coastal Range in eastern Taiwan, representing the first official record of amber from the mélange unit and as well as in Taiwan. The results, in addition to the affirmation of the amber, show that the amber is composed of sesquiterpenes and triterpenoids, indicating a possible origin of dipterocarp trees that are absent in the paleobotanic record and modern flora in Taiwan. Furthermore, infrared spectra analysis shows its compositional similarity to the amber from Sumatra, Indonesia, which boasts modern dipterocarp forests. Petrographic analysis of the surrounding sandstone suggests that the amber was deposited into the continental margin and allocated to Taiwan through the arc-continental collision in ~6–7 Ma. In summary, this study represents the first report of amber unearthed in the mélange unit and Taiwan. It shows that amber is a durable and reliable information carrier in accordance with biogeographic and tectonic evidence.

KEYWORDS

amber, resin, mélange, Taiwan, FTIR-ATR analysis, Petrographic analysis, Py-GC-MS analysis, Raman spectra analysis

1 Introduction

1.1 The occurrence of amber

Plants produce resinous secretion, which serves to heal injuries and obstruct predators (Labandeira, 2014). The resinous secretion is an organic material often highly resistant to weathering and thus is able to deposit in developing sediments. Throughout transportation, deep burial, thermal-pressure effect, and long-term maturation, the resin might transform into hard resin amber, and it is not regarded as a mineral due to the lack of a crystallographic structure. Moreover, before the eventual depositional place, transportation is a long-term process that takes

weeks to millennia (Labandeira, 2014). Typically, transportation from the source to the initial depositional area in a fluvial, lake, deltaic, lagoon, or nearshore marine environment, frequently, is from a few to tens of kilometers; much less commonly, a few hundred of kilometers (Martínez-Delclòs et al., 2004; Girard et al., 2008; Girard et al., 2009).

Due to the amber's botanical structural characteristics and composition (Anderson and Winans, 1991; Anderson et al., 1992) global amber classification system classified amber resinites into four classes. Class I is the most abundant, comprised of labdatriene carboxylic acids such as communic or ozic acids. The most famous origins are from the Baltic Sea, the Dominican Republic, and New Zealand. Class II resinites are formed from the polymer of bicycling sesquiterpenoid hydrocarbons and Triterpenoid. The most probable botanical affinity is Dipterocarpaceae, which is mainly distributed in the tropical forests of Southeast Asia. Class III, whose basic structural character is Polystyrene, was found in New Jersey and Germany, and the most probable botanical affinity is Hammelidaceae. Class IV resinites originate from Bovey-Tracy and Moravia, and the basic structural character is sesquiterpenoid, which is primarily based on the Cedrane skeleton.

In the present tropical rain forests of the Indian Peninsula and the Indo-China Peninsula, the Dipterocarpaceae is the dominant tree family and is one of the confirmed botanical provenances of the resinites (Anderson and Winans. (1991); Anderson et al., 1992). Dipterocarpaceae are also well known in Cenozoic fossil floras. Several fossils tension are recorded around the south, southeast, and east Asia regions, except in Taiwan, so far (Dutta et al., 2011; Rust et al., 2010; Böhme et al., 2013; Langenheim and Beck, 1965; Brackman et al., 1984; Van Aarssen et al., 1990; Kocsis et al., 2020; Hillmer et al., 1992; Feng et al., 2013; Shi et al., 2014; Naglik et al., 2018; Wang et al., 2018).

In this study, we first report and quantitatively analyze the amber resin of the family Dipterocarpaceae in Lichi Mélange at the southern tip of the Coastal Range, Eastern Taiwan. Moreover, it is also the first finding to report on the amber resin in the mélange unit. The chaotically tectonic origin of the Lichi Mélange and the arc-continental collision of Taiwan island implies the complicated journey and indeterminate era of resin production. This discovery fills the gap in the fossil record of the Dipterocarpaceae family in Taiwan and illustrates that the forearc basin gathers some tropical sediment sources far away from today's Taiwan island.

1.2 Geological background

Taiwan is an example of an ongoing arc-continental collisional orogeny produced by an oblique convergence between the passive

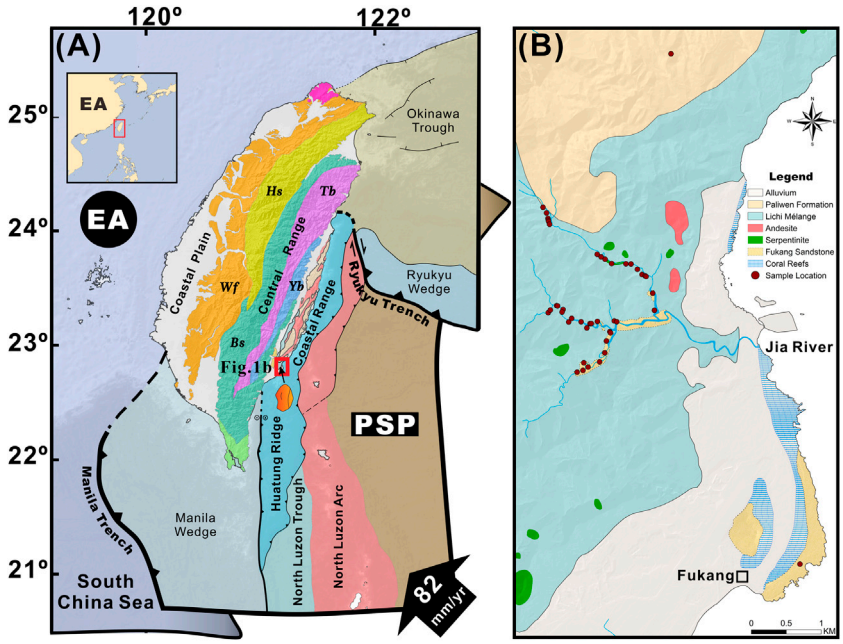

FIGURE 1
The tectonic and regional geological map of Taiwan. **(A)** Taiwan is an active arc-continental collision region in the junction of the Eurasian Plate (EA) and the Philippine Sea Plate (PSP). The south of Taiwan, the oceanic crust of the South China Sea (32–15 Ma), is subducted beneath the Philippine Sea Plate along the Manila Trench. To the east, the Philippine Sea Plate is subducted beneath the Eurasian plate along the Ryukyu trench and is moving northwestward at 310° at a rate of 82 mm/yr (Yu et al., 1997), colliding with the continental margin and forming the Coastal Range in Eastern Taiwan. To the southeastern offshore of Taiwan, the Huatung Ridge is a retrowedge ridge analogous to the Lichi Mélange; the forearc basin of the North Luzon Trough corresponds to the Plio-Pleistocene remnant forearc basins of the Coastal Range; the North Luzon Arc is equivalent to the Miocene volcanic units of the Coastal Range (modified from Lai et al., 2021; Malavieille et al., 2021). EA: Eurasian Plate; PSP: Philippine Sea Plate; *Wf*: Western Foothill; *Hs*: Hsuehshan slates; *Bs*: Backbone slates; *Tb*: Tailuko Belt (schists); *Yb*: Yuli Belt (schists) **(B)** The petrographic samples (red dots) are mainly collected from the sandstone blocks in Lichi Mélange in the Jia River drainage, Fukang sandstone near Fukang Fisher Harbor, and the Paliwen Formation in the northern part of the Jia River drainage, respectively. In this study area, the other large-scale exotic blocks (Serpentinite and Andesite) can also be found in Lichi Mélange (Modified from Lin et al., 2008).

continental margin of the Eurasian Plate and the Luzon volcanic arc on the Philippine Sea Plate (Chai, 1972; Suppe, 1981; Hayes and Lewis, 1984; Suppe, 1984; Tsai, 1986; Yu et al., 1997). The Eurasian Plate is adjacent to the South China Sea oceanic lithosphere southeastward that is subducted beneath the Philippine Sea Plate along the Manila trench, whereas the Philippine Sea Plate northward is subducted beneath the Eurasian Plate along the Ryukyu Trench (Figure 1A). The arc-continent collision is initiated at 5 Ma (e.g., Teng, 1990), with the onset increased in clastic sedimentation in Western and Eastern Taiwan, in the northern part of Taiwan and continuously propagates to the south.

The island of Taiwan consists of five morphotectonic units from west to east: the Coastal Plain, the Western Foothills, the Hsuehshan Range, the Central Range, and the Coastal Range. The Coastal Plain and Western Foothills consist of Pliocene to modern shallow marine siliciclastic deposits. The Hsuehshan Range and the western part of the Central Range are composed of Eocene to Miocene deep marine turbidites. The eastern part of the Central Range is featured by two metamorphic belts, including Tailuko and Yuli belts, which consist of the Paleozoic to the Mesozoic metamorphic basement and Oligocene to Miocene greenschist to blueschist facies, respectively. Lastly, the Miocene to Pliocene-accreted Tuluanshan volcanic arc and the Miocene to Pleistocene-deformed flysch forearc basins are exposed in the Coastal Range, Eastern Taiwan.

Eastern Taiwan is featured by the arc-continental collision along the Longitudinal Valley. Nowadays, with a length of approximately 150 km and a width of approximately 10 km, the Coastal Range is composed of four geological units: 1) the Miocene accreted volcanic arc of the Tuluanshan Formation, 2) the overlapped Plio-Pleistocene deformed sequence of unmetamorphosed flysch deposits, and the conglomerate of the Fanshuliao and Paliwen Formations, 3) the Miocene to Pleistocene chaotic disrupted blocks-in-matrix Lichi Mélange, and 4) the Pleistocene Peinanshan conglomerate (Hsu, 1956; Chang, 1967; Chang, 1969; Teng, 1987; Chen, 1988).

1.3 Lichi Mélange

"Mélange" is a term for mappable units of chaotic mixed rocks, including blocks of different lithology, origins, and ages (blocks-in-matrix) (Greenly, 1919; Festa et al., 2010). It is common to find the mélange unit at many collisional- and accretionary-type orogenic belts worldwide. In Taiwan, the Lichi Mélange, widely exposed along the southwestern flank of the Coastal Range, consists mainly of poorly stratified mudstone in which some large or small rock fragments or blocks of hard greyish sandstone, gabbro, serpentinite, and a minor slate are present (Hsu, 1956). Other exotic block lithologies include andesite, volcaniclastic rocks, limestone, ophiolite-bearing sedimentary rocks, amphibolite, low-grade meta-sandstones, and flysch blocks similar to the Fanshuliao and Paliwen formations scattered in the Lichi Mélange (Liou, 1977; Page and Suppe, 1981; Sung, 1991). The characteristic mesoscopic structure of the Lichi Mélange is that the curviplanar surfaces of the penetrative scaly foliation are generally polished and have aligned minerals and slickensides (Hsu, 1976; Teng, 1981; Chen, 1991; Chen, 1997; Chang et al., 2000; Chang et al., 2001). The origin of the Lichi Mélange is still debated. Prior studies have shown evidence of sedimentary (Liou, 1977; Page and Suppe, 1981) and tectonic processes (Chen, 1997; Chang et al., 2000; Chang et al., 2001) of the Lichi Mélange.

2 Materials and methods

The studied amber piece was collected from the broken sandstone blocks in the Jia River drainage (Figure 1B). Stratigraphically, it was unearthed from the Lichi Mélange at the southern tip of the Coastal Range (Figure 1). Embedded in a greyish sandstone matrix, the amber is yellowish and measures 1 cm in size (Figure 2). It is now reposited in the National Museum of Natural Science (NMNS, with catalog number NMNS 008480-F062389). To understand the origin and organic characteristics of the amber, this study performed a petrographic analysis of the matrix around the resin and the adjacent sandstone blocks to identify the sedimentary provenance.

In addition to the matrix around the amber, we also collected 45 sandstone blocks (43 samples along the Jia River drainage, one sample in the northern part of the Fukang fishing port, and one sample in the northern part of the Jia River drainage; Figure 1B). All the sandstone samples were block-in-matrix in sheared mudstone. The sedimentary facies are massive sandstone facies and thickly bedded-parallel laminated sandstone facies, and the samples were polarized for microscope observations, and we used Guzzi and Dickinson's method (Dickinson, 1970) to study the Q-F-L (quartz-feldspar-lithic fragment) diagram.

This study further implemented Raman spectroscopic analysis, FTIR-ATR, and Py-GC-MS to identify its organic characteristics. First, Raman spectra were obtained from an Enwave Prott-B2 in the Taiwan Union Lab of Gem Research. The near-infrared excitation is at 785 nm. Spectra were recorded at 1.6 cm^{-1} pixel resolution and 250–2,350 cm^{-1} in the spectral range.

Second, FTIR-ATR analysis was performed with a PerkinElmer FRONTIER FTIR at the Institute of Earth Sciences, National Ocean University. Spectra were collected from 4,000 to 400 cm^{-1}. The highest resolution was 0.4 cm^{-1}, and the common resolution was 4 cm^{-1}. The ATR accessory's spectra were collected from 4,000 to 400 cm^{-1}. The highest resolution was 0.4 cm^{-1}, and the common resolution was 4 cm^{-1}. Compared with traditional transmissive infrared analysis, this method has the advantages of high resolution, shorter analysis time, reduced sample pre-processing procedures, analysis of liquid and solid samples, and saving sample volume. The ratio of the integrated area of characteristics-absorbed wave provides a good way to distinguish the difference in provenance (Chen, 2019; Chen and Chang, 2020). The Factor (H) and Factor (O) are noted as follows:

$$Factor\,(H): \frac{CH_2\,(H) + CH_3\,(H)}{CH_2\,(H) + CH_3\,(H) + CH_3\,(L) + CH_2\,(L) + (C = C) + (C = O)} \quad (1)$$

$$Factor\,(O): \frac{(C = O)}{CH_2\,(H) + CH_3\,(H) + CH_3\,(L) + CH_2\,(L) + (C = C) + (C = O)} \quad (2)$$

Lastly, Py-GC-MS uses a sample heated to the point of molecular decomposition to characterize the resulting production of smaller biomolecules. A piece of the amber of less than 1 mg was sampled and ground into powder and was then prepared for the Pyrolysis-Gas Chromatography-Mass Spectrometry (Py-GC-MS) analysis.

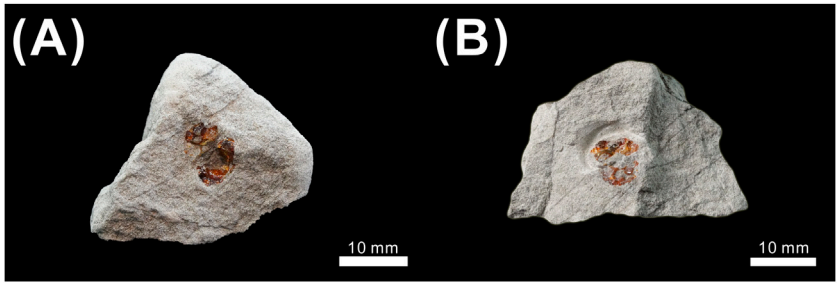

FIGURE 2
Fossil resin (amber) with wall rock from Lichi Mélange, Taiwan. The resin mosaic in the sandstone block in Lichi Mélange in Figure 1B and the yellowish resin show the transparent glassy occurrence.

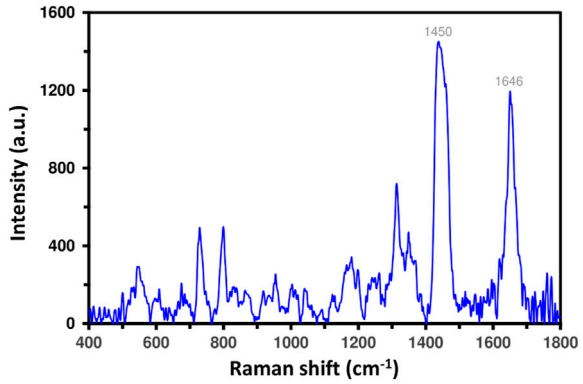

FIGURE 3
The Lichi amber Raman spectrum diagram. The Raman shift wavenumber is 400–1800 cm^{-1}, and at 1,450 and 1,646 cm^{-1}, has the strongest intensity peaks.

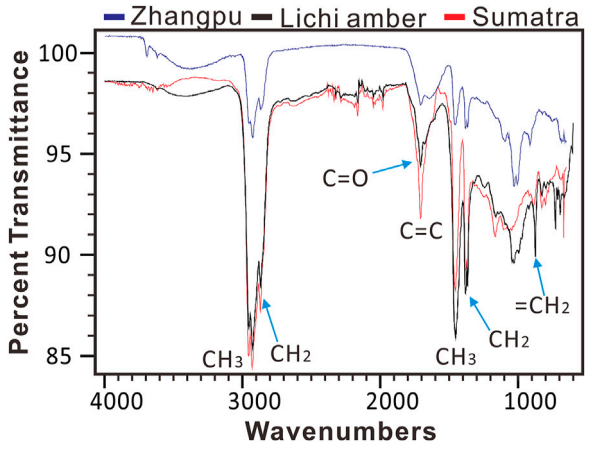

FIGURE 4
FTIR absorb spectra of amber samples from Zhangpu, Taiwan, and Sumatra. At 3,000–2,800 cm^{-1}, the absorbed peaks are CH_3 and CH_2 stretching vibrations; at 1,385–1,370 cm^{-1}, absorbed peaks are CH_2 bending vibration saturated hydrocarbon. At 887 cm^{-1}, the function group is exocyclic methylene. The blue, black, and red lines represent amber data from Zhangpu, Lichi, and Sumatra, respectively.

Py-GC-MS analyses were carried out using the Frontier PY-3030 Pyrolyzer system fitted to the Agilent 7890 GC which was coupled to the 7000 MS. The amber sample was loaded into a deactivated stainless steel sample cup and then pushed into the pyrolyzer by the autosampler. The initial pyrolysis temperature was set to 225°C. After heating at 225°C, the residue was then pyrolyzed at 300°C, 350°C, 380°C, 420°C, 450°C, and 600°C, with a heating rate of 20°C/min. The GC injector was held at 310°C, and the split mode was employed with a split ratio of 30:1. For the gas chromatographic separation, a Frontier UA-5 column (30 m × 0.25 mm i. d; 0.25 mm film thickness) was used. The carrier gas was operated in constant flow mode (He, purity 99.9995%) at 1.0 ml/min. The initial oven temperature was held at 40°C for 5 min then ramped to 300°C at a rate of 4°C/min, and then held for 20 min. The MS was operated in EI mode with an ionization energy of 70 eV; the transfer line was 310°C, and it was run in a scan mode (mass range 50–700 Da). The data processing was done with the MassHunter software, and the identification of compounds was based on the elution pattern and the comparison of mass spectra with the published works of literature. Py-GC-MS analylsis was performed in the Exploration and Development Research Institute, CPC Corporation, Taiwan.

3 Results and discussions

3.1 Characteristics of the Raman spectra

The result of the Raman spectra of the resin is shown in Figure 3. The most characteristic bands in the Raman spectrum of resin are the medium-strong and robust features at 1,646 and 1,450 cm^{-1}, respectively, which may be assigned to ν(C=C) stretching modes and δ(CH_2) deformation modes of characteristic peaks (Edward and Farwell, 1996; Brody et al., 2001). In the literature (Moreno et al., 2000; Brody et al., 2001; Winkler et al., 2001; Badea et al., 2015), the intensity ratio of the ν(C=C)/δ(CH_2) and I1646/I1450 is reported (Badea et al., 2015) to be indicative of the maturation process. The intensity ratio of the Lichi Amber is < 1 (0.82), owing to the degradation of the ν(C=C) unsaturation in the fossilized resin, probably through aerial or microbial oxidation (Edward and Farwell, 1996).

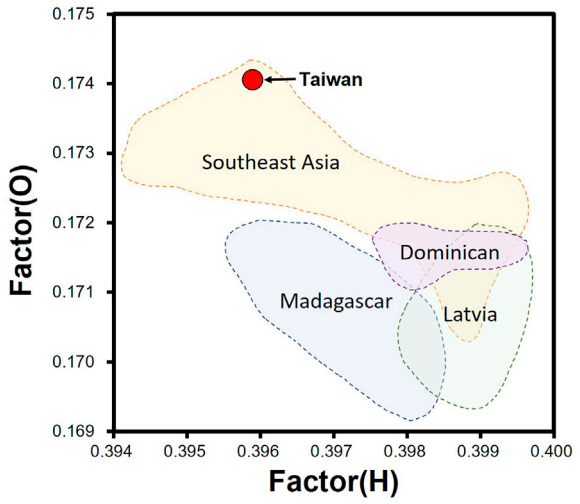

FIGURE 5
The origin of the different amber. Different color areas represent the different provenances of the amber. The yellow, blue, purple, and green area represent Southeast Asia, Madagascar, Dominican, and Latvia, respectively.

3.2 Characteristics of FTIR-ATR

The FTIR-ATR result of the Lichi Amber is shown in Figure 4. The wavenumbers 3000 to 2,800 cm^{-1} are saturated hydrocarbons for CH_3 and CH_2 stretching vibrations, and the wavenumbers 1385–1,370 cm^{-1} are CH_2 bending vibrations. With different origins and the amber's maturation process, the proportion of functional groups (C-H, C=C, and C=O bonds) will have different absorption ratios (Chen, 2019; Chen and Chang, 2020). In addition, the Lichi Amber sample has higher exocyclic methylene at 887 cm^{-1}, so it can be judged that the sample is less affected by heat or encounters short-buried history (Guiliano et al., 2007). Compared with different origins of amber (Chen, 2019; Chen and Chang, 2020; Chang and Chang, 2020; Chang, 2022; Chang et al., 2022), the pattern of the Lichi Amber has a high similarity with that of the Sumatra Amber. However, it shows a different proportion of functional groups from the pattern of the Zhangpu Amber, which is the closest geographic location. This result implies that the Lichi Amber might come from tropical Southeast Asia rather than the southeast of mainland China. The ratio of the empirical formula, Factor(H) *versus* Factor(O) (Figure 5), also shows the same result that the Lichi amber is correlated to the Southeast Asian amber (Chen, 2019; Chen and Chang, 2020; Chang and Chang, 2020; Chang, 2022; Chang et al., 2022).

3.3 Py-GC-MS result

Figure 6 shows the Py-GC-MS analysis pattern of the Lichi Amber. The amber contains sesquiterpenes, mainly Calamenene isomers, accompanied by β-amyrin, α-amyrin, and Hop-22 (29)-en-3β-ol triterpenoids. According to the composition of these terpenoids, the Lichi Amber in Lichi Mélange, Eastern Taiwan, belongs to the plants in the family of Dipterocarpaceae (Shi et al., 2014; Bonaduce et al., 2016; Chang and Chang, 2020; Chang et al., 2022; Simoneit et al., 2020).

3.4 The origin of the sandstone revealed by petrographic analysis

The petrography of the 46 sandstone blocks' samples in the southern tip of the Lichi Mélange shows two groups of different sandstone compositions (Figure 7A), which are the quartzose greywacke sandstone and the volcaniclastic sandstone. The quartzose greywacke mainly contains 65%–99% quartz, 0%–4% feldspar (mostly plagioclase), and 0%–34% lithic fragments. Under the thin section (Figure 7B), the quartz's angular and less polycrystalline quartz, which might come from the metamorphic rocks, can be found Moreover, the pyroclastic sandstone contains 2%–15% quartz, 78%–82% feldspar, and 5%–15% lithic fragment. In Figure 7C, the pyroclastic thin section shows that the quartz and plagioclase particles are angular. The petrographic result is similar to previous studies (Chen and Wang, 1988; Sung, 1991; Yang et al., 2012) and can be compared with the Type-I volcaniclastic sandstone and Type-II Quartzose-greywacke sandstone reported by Sung. (1991). The petrography of the amber's surrounding matrix also shows a Quartz-rich composition (quartz ~74.78%). However, limited by the insufficient number of samples collected, a single sample cannot summarize the most favorable preservation environment. This article is based on a single sample for observation and description. The petrographic studies show that most of the sandstone blocks in the Lichi Mélange are quartz-rich sandstones. Among the quartz granules, the primary source is from the low metamorphic facies region (Sung, 1991). Furthermore, most sandstone blocks belong to the turbidite facies; the original depositional environment also belongs to the deep-sea submarine fan of continental slopes or uplifts. Thus, the most numerous sandstone blocks in Lichi Mélange are from accretionary prisms from the Eurasian margin (Sung, 1991; Lai et al., 2021).

3.5 A hypothetical transportation route for Lichi amber

Through the Py-GC-MS and the biomarker, the polymer of bicycling sesquiterpenoid hydrocarbons and Triterpenoid indicated that the resin came from the Dipterocarpaceae species. The FTIR absorption spectrum shows that the pattern is more highly correlated to Sumatra's pattern than Zhangpu's pattern, implying that the source may come from tropical southeastern Asia. The petrographic and sedimentary facies analyses indicate that amber's wall rock source comes from deep-sea fans on the continental slope or continental uplift (Lai et al., 2021) at the margin of the Southeast Eurasia Plate.

The arc-continental collision between the Eurasian plate and the Luzon arc formed the history of the Taiwan orogenic belt and accumulated a variety origin of the sediment deposit in the forearc basin and was mixed in the Lichi Mélange from 15 to 5 Ma (Suppe, 1981; Teng, 1990; Chang et al., 2000, 2001). The Lichi amber, as one of the sources, comes from the southeastern Asia tropical forest, implying a fluke clue of a geomarker despite its lack of geochronological evidence. With several analyses in this study and the tectonic evolution of South China Sea rifting and the arc-continental collision of the Eurasian Plate and the Philippine Sea Plate, the hypothesis model is that (1) with the spreading of the

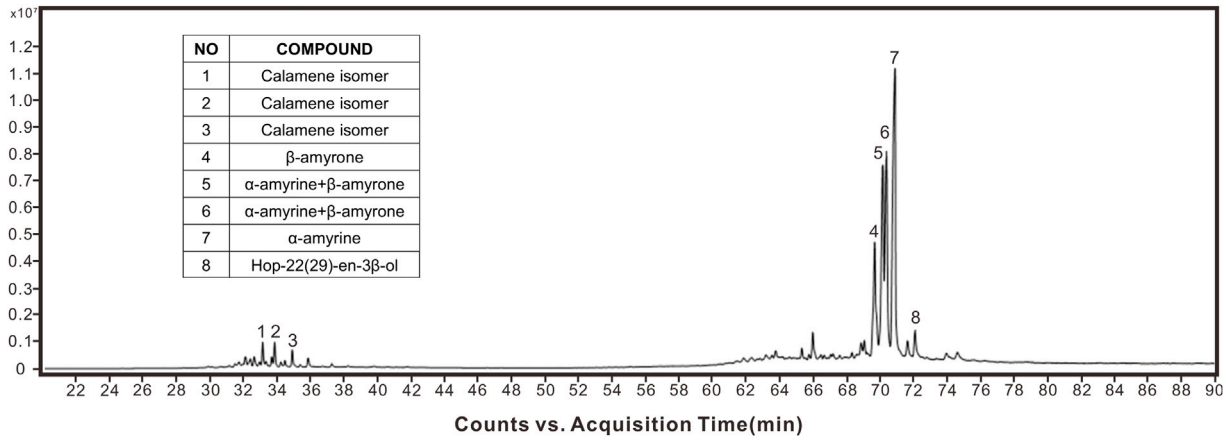

FIGURE 6
The total ion chromatogram of pyrolyzates of Lichi Amber at 350°C. Different peaks represent different organic matters. The identified compounds are listed in the top left of the pyrogram.

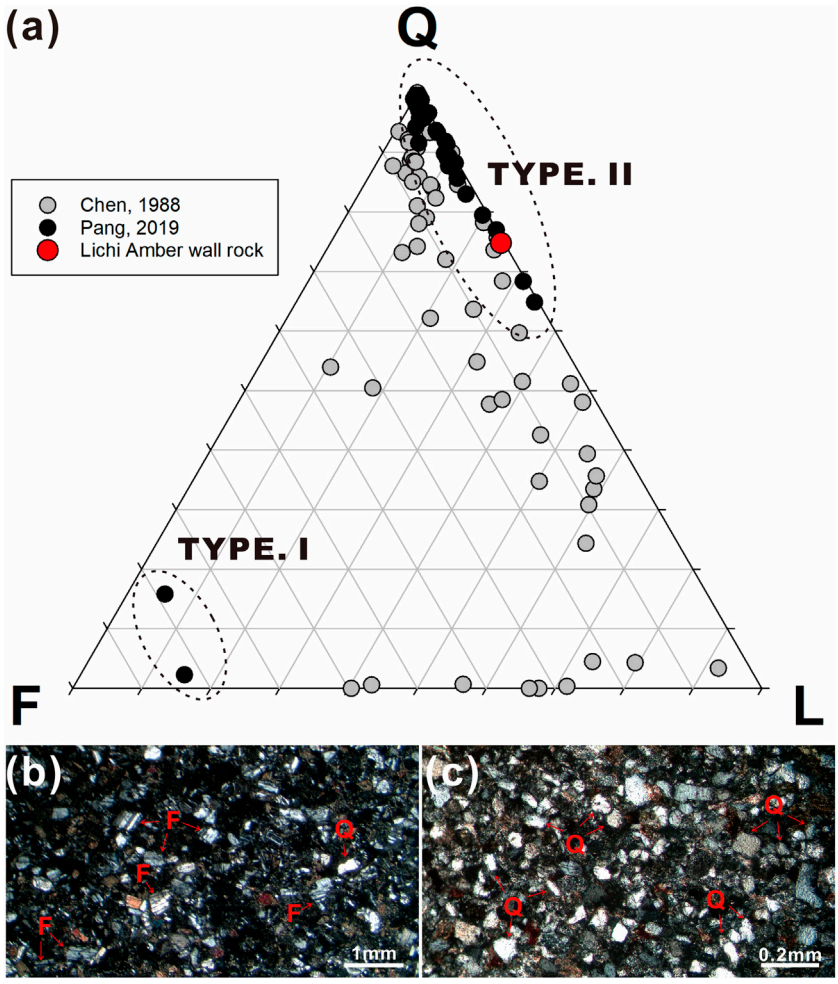

FIGURE 7
Sandstone Petrography and petrographic thin section in Lichi Mélange. All the sandstone block data are collected from Lichi Mélange (Chen, 1988; Pang, 2019). **(A)** Among the Q-F-L diagram, Q is quartz, F is a feldspar, and L is a lithic fragment. This diagram shows the proportion of three factors. **(B)** TYPE I is the feldspar-rich sandstone petrography, and **(C)** TYPE II is the quartz-rich sandstone petrography (Sung, 1991). The sources are mainly quartz-rich and lithic fragments. The feldspar-rich source is less. The gray circle is the data from Chen's (1988) sandstone blocks in Lichi Mélange. The black circle data are from Pang. (2019); the sampling location is displayed in Figure 2.

Dipterocarps from India since the Cretaceous (Khan et al., 2020), 2) the Dipterocarps migrated to the Southeast Asian rainforest in Neogene 3). The nannofossils study of the exotic blocks in Lichi Mélange suggested that the Lichi amber might form and transport from the Sumatra and associated regions to the basin and be preserved in sandstone on the continental slope or the continental uplift at the margin of the Eurasian Plate in 18–5.6 Ma (NN3-NN11, Chi, 1982) 4). From 5 Ma to the present, the sandstone and the amber slumped into the forearc basin, and during the arc-continental collision, the slumping or the shortening of the forearc basin with intensive shearing formed the Lichi Mélange and the amber was exposed to the surface (Suppe, 1981; Teng, 1990; Chang et al., 2000; Chang et al., 2001; Lai et al., 2021).

4 Conclusion

This study represents the first report on the unique amber resin from Taiwan. Raman spectra and FTIR-ATR analysis attribute the resin to the mature amber resinite. The FTIR absorption spectrum shows a great similarity between the studied amber and the amber from Sumatra, implying an origin from Southeastern Asia rather than the Chinese mainland. Revealed by Py-GC-MS analysis, the biomarkers such as sesquiterpenoid and triterpenoid suggest an origin from Dipterocarpaceae, which is commonly found in modern tropical Southeast Asia. Furthermore, although a single sample cannot directly assume the most favorable preservation environment and due to the complexity of the provenance of the mélange unit, we combined the result of the petrographic analysis with previous studies of sedimentary facies and tectonic evolution of the marginal Southeast Eurasian Plate and proposed a hypothesis transportation model of the amber.

Data availability statement

The raw data supporting the conclusion of this article will be made available by the authors, without undue reservation.

Author contributions

C-HP collected sandstone and discovered amber samples from Lichi regions. LL and C-HP designed this study. Y-JC, S-HL, and L-JS conducted FTIR-ATR, Raman spectra, and Py-GC-MS analyses, respectively. T-RY supported the biogeographic discussion and curated resin pictures. C-HP conducted petrographic analysis. C-TC and C-PC helped with field surveys, research funds, and research discussions. C-HP and LL prepared the first draft and all authors revised and improved it. All authors listed have made a substantial, direct, and intellectual contribution to the work and approved it for publication.

Funding

This work was financially supported by the National Science and Technology Council, Taiwan, under grant numbers: 105-2116-M-008-023 (C-PC); 107-2116-M-008-004 (C-TC); 109-2636-M-002-009 (LL); 109-2923-M-001-013-MY3, and 110-2116-M-001-004 (J-C, Lee).

Acknowledgments

The authors would like to thank Yi-Chun Hsu, Hou-Ping Ho, Hao-Cheng Sun, Xuan-Cheng Wei, Wan-Ching Chang Chien, and Chia-An Yue for helping with the field survey and sample collection; Kun-Wei Chung for helping to make the rock thin sections in the National Museum of Natural Science; and Yen-Yu Chen for helping with the FTIR-ATR analysis at the National Taiwan Ocean University.

Conflict of interest

The authors declare that the research was conducted in the absence of any commercial or financial relationships that could be construed as a potential conflict of interest.

Publisher's note

All claims expressed in this article are solely those of the authors and do not necessarily represent those of their affiliated organizations, or those of the publisher, the editors and the reviewers. Any product that may be evaluated in this article, or claim that may be made by its manufacturer, is not guaranteed or endorsed by the publisher.

References

Anderson, K. B., Winans, R. E., and Botto, R. E. (1992). The nature and fate of natural resins in the geosphere—II. Identification, classification and nomenclature of resinites. *Org. Geochem.* 18 (6), 829–841. doi:10.1016/0146-6380(92)90051-x

Anderson, K. B., and Winans, R. E. (1991). Nature and fate of natural resins in the geosphere. I. Evaluation of pyrolysis-gas chromatography mass spectrometry for the analysis of natural resins and resinites. *Anal. Chem.* 63 (24), 2901–2908. doi:10.1021/ac00024a019

Badea, G. I., Caggiani, M. C., Colomban, P., Mangone, A., Teodor, E. D., Teodor, E. S., et al. (2015). Fourier transform Raman and statistical analysis of thermally altered samples of amber. *Appl. Spectrosc.* 69 (12), 1457–1463. doi:10.1366/15-07866

Böhme, M., Aiglstorfer, M., Antoine, P. O., Antoine, P. O., Appel, E., Havlik, P., et al. (2013). A study of amber and copal samples using FT-Raman spectroscopy. *Zitteliana. Reihe A, Mitteilungen der Bayerischen Staatssammlung für Paläontologie und Geologie* 53, 121–167.

Bonaduce, I., Di Girolamo, F., Corsi, I., Degano, I., Tinè, M. R., and Colombini, M. P. (2016). Terpenoid oligomers of dammar resin. *Journal of Natural Products* 79 (4), 845–856.

Brackman, W., Spaargaren, K., Van Dongen, J. P. C. M., Couperus, P. A., and Bakker, F. (1984). Origin and structure of the fossil resin from an Indonesian Miocene coal. *Geochimica et Cosmochimica Acta* 48 (12), 2483–2487.

Brody, R. H., Edwards, H. G., and Pollard, A. M. (2001). A study of amber and copal samples using FT-Raman spectroscopy. *Spectrochimica Acta Part A Mol. Biomol. Spectrosc.* 57 (6), 1325–1338. doi:10.1016/s1386-1425(01)00387-0

Chai, B. H. (1972). Structure and tectonic evolution of Taiwan. *Am. J. Sci.* 272 (5), 389–422. doi:10.2475/ajs.272.5.389

Chang, C. P., Angelier, J., Huang, C. Y., and Liu, C. S. (2001). Structural evolution and significance of a mélange in a collision belt: The Lichi mélange and the taiwan arc–continent collision. *Geol. Mag.* 138 (6), 633–651. doi:10.1017/s0016756801005970

Chang, C. P., Angelier, J., and Huang, C. Y. (2000). Origin and evolution of a mélange: The active plate boundary and suture zone of the Longitudinal Valley, taiwan. *Tectonophysics* 325 (1-2), 43–62. doi:10.1016/s0040-1951(00)00130-x

Chang, L. S. (1969). A biostratigraphic study of the Tertiary in the Coastal Range, eastern Taiwan, based on smaller foraminifera (III. Middle Part). *Proc. Geol. Soc. China* 12, 89–101.

Chang, L. S. (1967). A biostratigraphic study of the Tertiary in the Coastal Range, eastern Taiwan, based on smaller foraminifera (I. Southern Part). *Proc. Geol. Soc. China* 10, 64–76.

Chang, S. C. (2022). Terpenoid biomarkers and botanical affinity of fossil resins. Master thesis. Keelung, Taiwan: National Taiwan Ocean University, 95

Chang, S. C., and Chang, Y. J. (2020). Terpenoid compositions and botanical origins of fossil resin from Indonesia and Dominican. *J. Natl. Taiwan Mus.* 73 (1), 17–26.

Chang, S. C., Chang, Y. J., and Shiau, L. J. (2022). Terpenoid composition and infrared spectroscopy of detarioideae hymenaea Origin of Fossil Resin. *J. Natl. Taiwan Mus.* 75 (3), 43–57.

Chen, W. S., and Wang, Y. (1988). The plio-pleistocene basin development in the coastal range of taiwan. *ACTA Geol. Taiwanica* 26, 37–56.

Chen, W. S. (1997). Mesoscopic structures developed in the Lichi Mélange during the arc–continent collision in the Taiwan region. *J. Geol. Soc. China* 40, 415–434.

Chen, W. S. (1991). Origin of the Lichi mélange in the coastal range, eastern taiwan. *Special Publ. Central Geol. Surv.* 5, 257–266.

Chen, W. S. (1988). Tectonic evolution of sedimentary basins in the coastal range, eastern taiwan. (Unpublished Ph.D. thesis). Taipei, Taiwan: National Taiwan University, 304.

Chen, Y. Y. (2019). Application of FTIR-ATR spectroscopy to the characterization of chemical functional groups in organic matter. Master thesis. Keelung, Taiwan: National Taiwan Ocean University, 90.

Chen, Y. Y., and Chang, Y. J. (2020). Applications of FTIR-ATR spectroscopy in the analysis of organic chemical functional groups. *J. Natl. Taiwan Mus.* 73 (1), 1–16.

Chi, W. R. (1982). The calcareous nannofossils of the Lichi Mélange and the Kenting Mélange and their significance in the interpretation of plate-tectonics of the Taiwan region. *Ti-Chih* 4, 99–114.

Dickinson, W. R. (1970). Interpreting detrital modes of graywacke and arkose. *J. Sediment. Res.* 40 (2), 695–707.

Dutta, S., Mallick, M., Kumar, K., Mann, U., and Greenwood, P. F. (2011). Terpenoid composition and botanical affinity of Cretaceous resins from India and Myanmar. *Int. J. Coal Geol.* 85 (1), 49–55. doi:10.1016/j.coal.2010.09.006

Edwards, H. G., and Farwell, D. W. (1996). Fourier transform-Raman spectroscopy of amber. *Spectrochimica Acta Part A Mol. Biomol. Spectrosc.* 52 (9), 1119–1125. doi:10.1016/0584-8539(95)01643-0

Feng, X., Tang, B., Kodrul, T. M., and Jin, J. (2013). Winged fruits and associated leaves of Shorea (Dipterocarpaceae) from the Late Eocene of South China and their phytogeographic and paleoclimatic implications. *Am. J. Bot.* 100 (3), 574–581. doi:10.3732/ajb.1200397

Festa, A., Pini, G. A., Dilek, Y., and Codegone, G. (2010). Mélanges and mélange-forming processes: a historical overview and new concepts. *International Geology Review* 52, 1040–1105.

Girard, V., Schmidt, A. R., Saint Martin, S., Struwe, S., Perrichot, V., Saint Martin, J. P., et al. (2008). Evidence for marine microfossils from amber. *Proc. Natl. Acad. Sci.* 105 (45), 17426–17429. doi:10.1073/pnas.0804980105

Girard, V., Schmidt, A. R., Struwe, S., Perrichot, V., Breton, G., and Néraudeau, D. (2009). Taphonomy and palaeoecology of mid-Cretaceous amber-preserved microorganisms from southwestern France. *Geodiversitas* 31 (1), 153–162. doi:10.5252/g2009n1a14

Greenly, E. (1919). The geology of angelsey: great britain geol. *Survey Mem.* 98.

Guiliano, M., Asia, L., Onoratini, G., and Mille, G. (2007). Applications of diamond crystal ATR FTIR spectroscopy to the characterization of ambers. *Spectrochimica Acta Part A Mol. Biomol. Spectrosc.* 67 (5), 1407–1411. doi:10.1016/j.saa.2006.10.033

Hayes, D. E., and Lewis, S. D. (1984). A geophysical study of the Manila trench, Luzon, Philippines: 1. Crustal structure, gravity, and regional tectonic evolution. *J. Geophys. Res. Solid Earth* 89 (B11), 9171–9195. doi:10.1029/jb089ib11p09171

Hillmer, G., Weitschat, S. W., and Vávra, N. (1992). Bernstein aus dem Miozän von Borneo. *Naturwissenschaftliche Rundschau* 45 (2), 72–74.

Hsu, T. L. (1956). Geology of the coastal range, eastern taiwan. *Bull. Geol. Surv. Taiwan* 8, 15–41.

Hsu, T. L. (1976). The Lichi mélange in the coastal range framework. *Bull. Geol. Surv. Taiwan* 25, 87–95.

Khan, M. A., Spicer, R. A., Spicer, T. E., Roy, K., Hazra, M., Hazra, T., et al. (2020). Dipterocarpus (Dipterocarpaceae) leaves from the K-pg of India: A cretaceous gondwana presence of the Dipterocarpaceae. *Plant Syst. Evol.* 306 (6), 90–18. doi:10.1007/s00606-020-01718-z

Kocsis, L., Usman, A., Jourdan, A. L., Jumat, N., Daud, D., Briguglio, A., et al. (2020). The Bruneian record of "Borneo Amber": a regional review of fossil tree resins in the Indo-Australian Archipelago. *Earth-Science Reviews* 201, 103005.

Labandeira, C. C. (2014). Amber. *Paleontological Soc. Pap.* 20, 163–216. doi:10.1017/s1089332600002850

Lai, L. S. H., Dorsey, R. J., Horng, C. S., Chi, W. R., Shea, K. S., and Yen, J. Y. (2021). Polygenetic mélange in the retrowedge foredeep of an active arc-continent collision, Coastal Range of eastern Taiwan. *Sediment. Geol.* 418, 105901. doi:10.1016/j.sedgeo.2021.105901

Langenheim, J. H., and Beck, C. W. (1965). Infrared spectra as a means of determining botanical sources of amber. *Science* 149 (3679), 52–55. doi:10.1016/j.sedgeo.2021.105901

Lin, W. H., Lin, C. W., Liu, Y. C., and Chen, P. T. (2008). *Geological map of taitung and jhihben, sheet map 59 and 64 (scale 1:50,000).* Taipei, Taiwan: Central Geological Survey, MOEA, ROC.

Liou, J. G. (1977). *The East Taiwan Ophiolite: Its occurrence, petrology, metamorphism, and tectonic setting.* United States: Mining Research and Service Organization, 1–213.

Malavieille, J., Dominguez, S., Lu, C. Y., Chen, C. T., and Konstantinovskaya, E. (2021). Deformation partitioning in mountain belts: Insights from analogue modelling experiments and the taiwan collisional orogen. *Geol. Mag.* 158 (1), 84–103. doi:10.1017/s0016756819000645

Martı´nez-Delclòs, X., Briggs, D. E., and Peñalver, E. (2004). Taphonomy of insects in carbonates and amber. *Palaeogeogr. Palaeoclimatol. Palaeoecol.* 203 (1-2), 19–64. doi:10.1016/s0031-0182(03)00643-6

Moreno, Y. M., Christensen, D. H., and Nielsen, O. F. (2000). A NIR-FT-Raman spectroscopic study of amber. *Asian J. Spectrosc.* 4 (2), 49–56.

Naglik, B., Kosmowska-Ceranowicz, B., Natkaniec-Nowak, L., Drzewicz, P., Dumańska-Słowik, M., Matusik, J., et al. (2018). Fossilization history of fossil resin from Jambi Province (Sumatra, Indonesia) based on physico-chemical studies. *Minerals* 8 (3), 95. doi:10.3390/min8030095

Page, B. M., and Suppe, J. (1981). The Pliocene Lichi mélange of Taiwan; its plate-tectonic and olistostromal origin. *Am. J. Sci.* 281 (3), 193–227. doi:10.2475/ajs.281.3.193

Pang, C. H. (2019). Structural evolution of Lichi mélange in southern tip of the coastal range, taiwan. (Master thesis). Taoyuan, Taiwan: National Central University, 122.

Rust, J., Singh, H., Rana, R. S., McCann, T., Singh, L., Anderson, K., et al. (2010). Biogeographic and evolutionary implications of a diverse paleobiota in amber from the early Eocene of India. *Proceedings of the National Academy of Sciences* 107 (43), 18360–18365.

Shi, G., Dutta, S., Paul, S., Wang, B., and Jacques, F. M. (2014). Terpenoid compositions and botanical origins of Late Cretaceous and Miocene amber from China. *PLoS One* 9 (10), e111303. doi:10.1371/journal.pone.0111303

Simoneit, B. R., Oros, D. R., Karwowski, Ł., Szendera, Ł., Smolarek-Lach, J., Goryl, M., et al. (2020). Terpenoid biomarkers of ambers from Miocene tropical paleoenvironments in Borneo and of their potential extant plant sources. *International Journal of Coal Geology*, 103430.

Sung, Q. (1991). Depositional mechanism of the Fukang sandstone, Lichi mélange, eastern taiwan. *Proc. Geol. Soc. China* 34, 173–198.

Suppe, J. (1984). Kinematics of arc-continent collision, flipping of subduction, and back-arc spreading near Taiwan. *Mem. Geol. Soc. China* 6, 21–33.

Suppe, J. (1981). Mechanics of mountain building and metamorphism in Taiwan. *Mem. Geol. Soc. China* 4 (6), 67–89.

Teng, L. S. (1990). Geotectonic evolution of late Cenozoic arc-continent collision in Taiwan. *Tectonophysics* 183 (1-4), 57–76. doi:10.1016/0040-1951(90)90188-e

Teng, L. S. (1981). Island arc system of the coastal range, eastern taiwan. *Proc. Geol. Soc. China* 24, 99–112.

Teng, L. S. (1987). Tectostratigraphic facies and geologic evolution of the coastal range, eastern taiwan. *Mem. Geol. Soc. China* 8, 229–250.

Tsai, Y. B. (1986). Seismotectonics of taiwan. *Tectonophysics* 125, 17–37. doi:10.1016/0040-1951(86)90005-3

Van Aarssen, B. G. K., Cox, H. C., Hoogendoorn, P., and De Leeuw, J. W. (1990). A cadinene biopolymer in fossil and extant dammar resins as a source for cadinanes and bicadinanes in crude oils from South East Asia. *Geochimica et Cosmochimica Acta*, 54 (11), 3021–3031.

Wang, H., Dutta, S., Kelly, R. S., Rudra, A., Li, S., Zhang, Q. Q., et al. (2018). Amber fossils reveal the Early Cenozoic dipterocarp rainforest in central Tibet. *Palaeoworld* 27 (4), 506–513. doi:10.1016/j.palwor.2018.09.006

Winkler, W., Kirchner, E. C., Asenbaum, A., and Musso, M. (2001). A Raman spectroscopic approach to the maturation process of fossil resins. *J. Raman Spectrosc.* 32 (1), 59–63. doi:10.1002/1097-4555(200101)32:1<59:aid-jrs670>3.0.co;2-d

Yang, X. C., Li, K. H., and Chen, W. S. (2012). The application of petrographic analysis to archaeological research: Examples from the artifacts and sherds of chiu hsiang lan site, taitung, taiwan. *J. Austronesian Stud.* 3 (2), 71–88.

Yu, S. B., Chen, H. Y., and Kuo, L. C. (1997). Velocity field of GPS stations in the Taiwan area. *Tectonophysics* 274 (1-3), 41–59. doi:10.1016/s0040-1951(96)00297-1